Greenland Ice Sheet Memory for Cloud Radiation determines its impact on the Surface Mass Balance

M. Izeboud[1], S. Lhermitte[1], K. Van Tricht[2], J.T.M. Lenaerts[3], N. Van Lipzig[4], N. Wever[3]

[1]Delft University of Technology, Department of Geoscience and Remote Sensing
[2]VITO Remote Sensing, Mol, Belgium
[3]Department of Atmospheric and Oceanic Sciences, University of Colorado Boulder, Boulder CO, USA
[4]KU Leuven
[1]Stevinweg 1, 2628CN Delft, The Netherlands
[2]Boeretang 200, 2400 Mol, Belgium
[3]311 UCB, Boulder, Colorado, 80309-0311, United States of America
[4]Oude Markt 13, 3000 Leuven, Belgium

Key Points:

- The cloud radiative effect on the GrIS shows a strong but always positive seasonal cycle
- The short-term ice sheet response to cloud radiation is a reduction of surface melt
- The long-term response is opposite with increased surface melt through a decreased surface albedo

Corresponding author: M. Izeboud, `maaike.izeboud@live.nl`

Abstract

As of yet, there is no consensus on the role of the cloud radiative effect (CRE) on the Greenland Ice Sheet (GrIS). This study focuses on the seasonal and temporal variability of the CRE, to better understand the response of the firn. To do so, we combine satellite observations, climate-model output, and a snow model. We separate short-term and long-term impacts. The results show a positive CRE for all seasons, with an annual short-term CRE of 24.7 Wm^{-2}, which is largest in fall. The long-term response of the GrIS to the CRE is positive and dominant in summer ablation areas, decreasing the albedo and enhancing melt-water runoff. This long-term effect stresses the influence of the firn conditions on its response to CRE, and highlights the need to include a snow model to study GrIS cloud radiation. The (lack off) long-term component of the CRE explains the conflict in previous studies.

1 Introduction

The Greenland Ice Sheet (GrIS) has been losing mass since the late 1990's through a rise in surface meltwater runoff (Fettweis, Franco, et al., 2013; van den Broeke et al., 2016) that results from an increase in atmospheric temperatures. The rise in meltwater runoff is mainly attributed to atmospheric changes, with more frequent warm and dry summers (Fettweis, Hanna, et al., 2013), and a decrease in surface albedo (Box et al., 2012). Arctic clouds trigger feedback mechanisms that induce albedo changes and regulate surface melt principally because clouds regulate the amount of radiation received by the surface (Bintanja & Van Den Broeke, 1996). Over Polar Regions, including the GrIS, the increase in longwave (LW) radiation dominates the decrease in shortwave (SW) radiation, leading to a net positive cloud radiative effect (CRE) on annual time scales. This affects the conditions of the GrIS firn, reducing meltwater refreezing and thereby accelerating bare-ice exposure (decreasing the albedo) and enhancing meltwater runoff (van Tricht et al., 2016). However, Hofer et al. (2017) argue that the observed decreasing summer cloud cover, i.e. a relative increase in SW radiation, is the main driver for meltwater runoff. Furthermore, Wang et al. (2018) argue that clouds stabilize the albedo feedback and decelerate surface melt, referring to a net negative CRE observed by automatic weather stations (AWS).

The main motivation to study the response of the GrIS to cloud radiation more closely, is to better understand these conflicting views on the impact of CRE. This is done by gaining insight in the seasonal variability of the CRE and to seek what the long term effect of clouds are. This is done by gaining insight in the seasonal variability of the CRE and to quantify the long term and short terms effects of clouds on the GrIS. Therefore, we adopt the methodology of van Tricht et al. (2016): we use CloudSat-CALIPSO satellite remote sensing observations of cloud conditions over the period 2007 to 2010, which are complemented by atmospheric data from a regional climate model (RACMO2.3) to create a realistic cloud forcing dataset with hourly temporal resolution. The reason to adopt their method is twofold: it uses a dataset that has both high spatial and temporal resolution, and it includes a snow model that allows to study the cloud-surface interaction. With more detailed SNOWPACK simulations, that can be compared on a day to day basis, the GrIS CRE can be assessed for separate seasons and the short-term and long-term response of the snowpack to radiative forcing can be quantified separately.

The CRE (Wm^{-2}) is defined as the difference in net radiation fluxes of an all-sky scenario to a clear-sky scenario simulation, defined in equation 1. A positive CRE indicates net cloud warming at the surface; a negative CRE indicates net cloud cooling. The all-sky scenario provides the observation based estimate of the GrIS meteorology. In the clear-sky scenario, all clouds and their radiative effects are removed. Precipitation (both solid and liquid) is left unchanged to exclude other changes in the atmosphere and snowpack. The magnitude of the radiative effect is intimately connected to the amount of ice and liquid water in the cloud, its temperature, solar zenith angle and surface albedo (Shupe & Intrieri, 2004).

$$CRE = F^{\downarrow\uparrow}_{SW,all-sky} + F^{\downarrow\uparrow}_{LW,all-sky} - \left(F^{\downarrow\uparrow}_{SW,clear-sky} + F^{\downarrow\uparrow}_{LW,clear-sky}\right) \tag{1}$$

2 Methods and Data

The methodology used in this study is based on van Tricht et al. (2016), see their paper in *Nature Communications (doi 10.1038/ncomms10266)* for a detailed explanation. Simulations are performed with the physically-based snow model SNOWPACK (Lehning et al., 2002) to assess the impact of the cloud CRE on surface snow and firn conditions. A state-of-the-art hybrid dataset has been created to represent the cloud forcing on the GrIS surface mass balance (SMB). This hybrid data set is a combination of CloudSat-CALIPSO satellite observations and data from the regional climate model, RACMO2.3 (Noel, 2015). The combination of the data sets creates a much needed observation-based dataset, that also has a high temporal resolution. The hybrid data set has been evaluated by ground-based observations and automatic weather stations (AWSs) and proved to perform better than just the climate model data. The same hybrid data set is used to force SNOWPACK in this study.

2.1 SNOWPACK simulations

SNOWPACK (Lehning et al., 2002) is a one-dimensional physical snow and land-surface model, which focuses on a detailed description of the mass and energy exchange between the snow and the atmosphere. Here we use SNOWPACKs to account for processes that are not included in the satellite products: the response of the GrIS to the excess energy of the CRE. To better represent GrIS snow conditions, SNOWPACK has been refined to include a prognostic snow albedo parameterization (van Angelen, 2012; Gardner & Sharp, 2010) that accounts for snow grain size variations, cloud optical depth, solar zenith angle and concentration of light-absorbing impurities at the surface. van Tricht et al. (2016) has shown that, with the albedo scheme implemented, SNOWPACK performs well in simulating GrIS surface conditions.

To couple the effect of clouds on the surface energy balance (SEB) to the SMB, SNOWPACK simulations were performed for an all-sky and clear-sky scenario on a 2° by 2° grid for the three consecutive hydrological years, from September 2007 to September 2010. The all-sky scenario provides the most observation based estimate of the actual GrIS CRE. In the clear-sky scenario, all clouds and their radiative effects are removed. Note that precipitation (both solid and liquid) is left unchanged to exclude other changes in the atmosphere and snowpack.

2.2 Scenarios

To create insight in the temporal variability of the CRE, each day in the three hydrological years is simulated individually. This approach enables us to initialize each day for different scenarios. With this we simulate more scenario's than van Tricht et al. (2016), whom initialized only at the start of the simulation (2007). Now, each day is initialized with preceding either only all-sky conditions (AI) or only clear-sky conditions (CI). For both the all-sky initialization scheme and clear-sky initialization scheme, each day is simulated twice: once for an all-sky day (A) and once for a clear-sky (C) day. Consequently, there are four scenarios using this approach:

1. AAI: one all-sky day simulated, initialised with preceding all-sky conditions. This is the most observation based scenario, including all clouds that have occurred.
2. CAI: one clear-sky day simulated, initialised with preceding all-sky conditions.

3. ACI: one all-sky day simulated, initialised with preceding clear-sky conditions.
4. CCI: one clear-sky day simulated, initialised with preceding clear-sky conditions. This is the scenario where no clouds occur, ever.

These four scenarios allow to separate between short and long-term cloud effects. The following comparisons are made:

(a) Short-term cloud radiative effect: difference between scenario AAI-CAI and scenario ACI-CCI. These schemes have the same initial firn conditions, but different cloud forcing for one day.
(b) Long-term cloud radiative effect: difference between scenario AAI-ACI and scenario CAI-CCI. These schemes enjoy the same daily forcing but different initial firn conditions.

3 Results

3.1 Seasonal variations of Cloud Radiative Effect

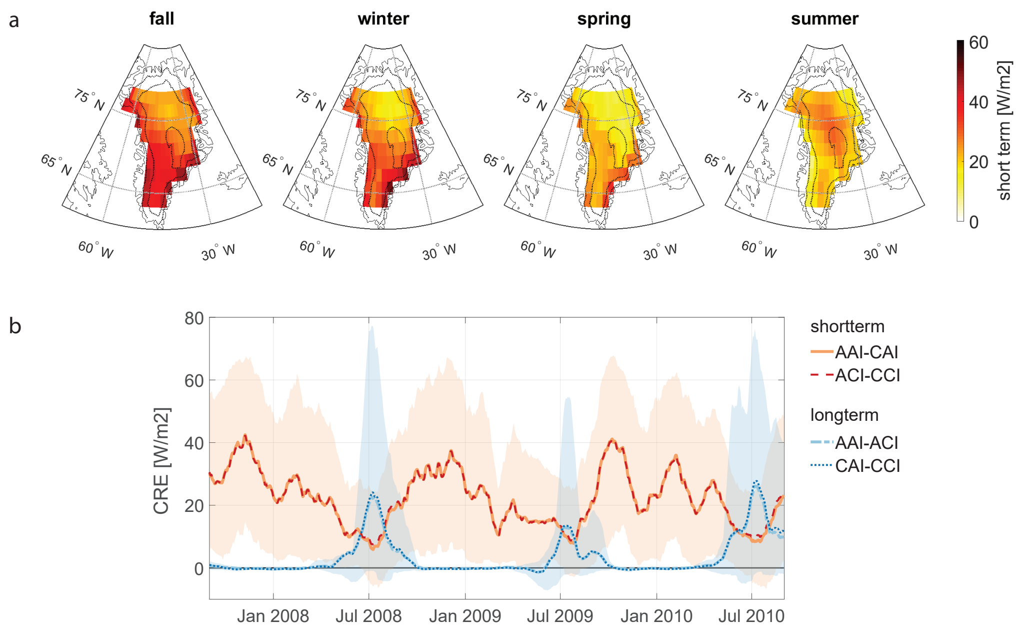

Figure 1. Cloud radiative effect (CRE) on the GrIS. a) Short-term CRE per season, averaged difference between scenario AAI-CAI and ACI-CCI over 2007-2010. Values per grid point are seasonal averages. b) Time-series of both short-term (red lines, scenario AAI-CAI and ACI-CCI) and long-term (blue lines, scenario AAI-ACI and CAI-CCI) CRE, for only ablation grid points. Plotted with a 30-day moving average. The shaded areas represent the 10 to 90 percentile of the ablation gridpoint data.

The simulations show that clouds have a net positive radiative impact, for all season in the year. See figure 1. There are a few strong ablation gridpoints that are an exception to this, but for a such limited period of time in summer that no monthly averaged CRE is negative. For the two comparison cases the annual averages for the GrIS are a) short-term (scenario AAI-CAI) 24.8 $\pm 2.5 \mathrm{Wm}^{-2}$ and (scenario ACI-CCI) 24.8$\pm 2.4 \mathrm{Wm}^{-2}$, b) long-term (scenario AAI-ACI) 0.6 $\pm 5.4 \mathrm{Wm}^{-2}$ and (scenario CAI-CCI) 0.6 $\pm 5.3 \mathrm{Wm}^{-2}$

respectively. The direct atmospheric CRE, without any snow feedback, is $29.5 Wm^{-2}$ (van Tricht et al., 2016). Following the timescale from direct to long-term, the annual average CRE decreases. These differences show that the GrIS buffers the positive CRE. The differences between the two short-term or respectively long-term components is small, showing that the short-term CRE is not highly affected by the GrIS initialisation and that the long-term CRE does not change a great deal for different daily forcing. As the distinction between short-term and long-term is both more significant and of more interest, the differences between the components of each time scale are not included in further analysis. The small difference of the components allows to average them for spatial visualisation in figure 1a.

The short-term CRE (figure 1a) is stronger than the long-term CRE (figure 1b), and its maximum is in fall with GrIS average $31.4 \pm 1.5\mathrm{Wm}^{-2}$, and the minimum effect is in spring, $19.4 \pm 1.8\mathrm{Wm}^{-2}$. Furthermore, the ablation grid points, located along the coasts, and the south area on the GrIS show a more pronounced seasonal fluctuation than the inland. A negative, short-term CRE occurs at some grid points in summer, but this is never prevalent. Each grid point has a monthly positive CRE.

The the mangitude of the annual long-term CRE is smaller than the short-term CRE, whereas its spatial behaviour is similar to the short-term CRE (not shown). A strong peak of long-term CRE can be seen in summer, but only for ablation grid points. For accumulation grid points (inland), the long-term CRE is negligible compared to it's accompanying short-term CRE (supplementary figure S1). The positive long-term CRE indicates that the GrIS has a memory for its preceding conditions and that clouds have a lasting net warming effect. The figure shows that this memory does not extend to other seasons, indicating that the memory of the GrIS in terms of radiation energy is no longer than 1-3 months. Nevertheless, during the melt season, this CRE memory is key as the long-term CRE is dominant over the short-term CRE. The short-term CRE goes down, due to SW cloud cooling, but the long-term CRE goes up. Note that only the short-term CRE is measurable, whereas the long-term GrIS response can only be determined by a snow model. All in all, this positive long-term CRE component suggest that persistent cloud cover has an important role on the GrIS SMB forcing, or related to this: that the state of the GrIS is essential for cloud radiation studies.

3.2 Response of GrIS to Cloud Radiative Forcing

The response of the GrIS to cloud radiative forcing is our main interest. As previously stated, the GrIS buffers the radiative energy on a daily time scale and, in summer, even for longer time scales.

On short-term time scale, the positive CRE induces surface warming (supplementary figure S2). The annual averages for the surface warming due to cloud radiation on the GrIS are $1.0 \pm 0.3\mathrm{Wm}^{-2}$ (scenario AAI-CAI) and $1.1 \pm 0.4\mathrm{Wm}^{-2}$ (scenario ACI-CCI). The spatial and temporal variations of the surface warming are closely correlated to the CRE. The net SW radiation, figure 2b, decreases in cloudy conditions, but not enough to induce net cloud cooling (CRE < 0). The short-term effect of clouds on the albedo is positive as a result of the broadband albedo increase in cloudy conditions (Gardner & Sharp, 2010), but as this is embedded in the albedo parameterization it cannot be stated to be solely the response of the GrIS (figure 2c).

The long-term CRE increases in summer due to an increased storage of net SW radiation, as opposed to the decrease of SW radiation on short time scales. The opposing response was never quantified before, as only the direct differences in SW radiation can be measured, and illsutrates the importance of accounting for the long term response.. The positive effect of clouds on the net SW budget can be explained by the accompanying decrease in albedo, allowing for more absorbed radiation. This in turn increases the surface melt rates (visualized as a negative cloud effect on snow water equivalent (SWE),

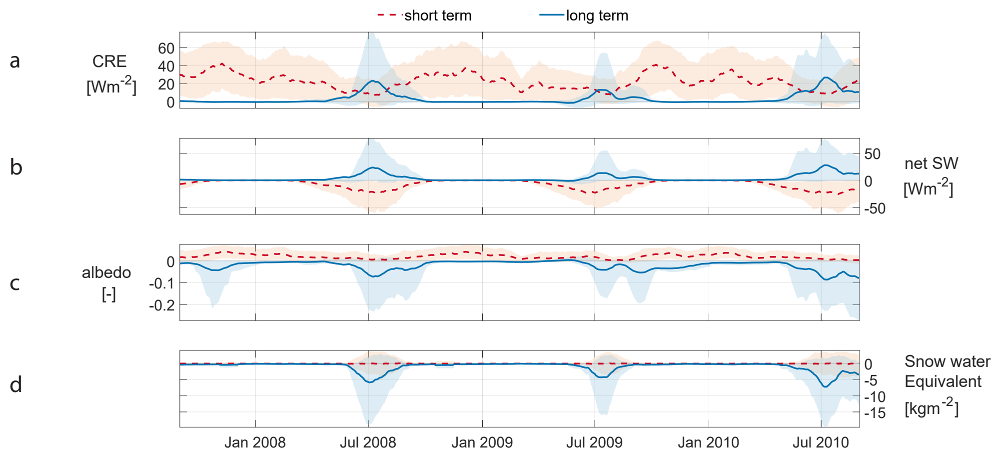

Figure 2. Cloud effect on the GrIS ablation grid points for different variables, plotted with a 30-day average. The shaded areas represent the 10 to 90 percentile of the ablation gridpoint data. Time series of both short-term (red dashed line, average of scenario AAI-CAI and ACI-CCI) and long-term (blue line, average of scenario AAI-ACI and CAI-CCI) cloud effect. a) Cloud Radiative effect, b) Cloud effect on net shortwave radiation, c) Cloud effect on surface albedo, d) Cloud effect on snow water equivalent.

figure 2d). When surface melt starts to occur, the albedo drops even lower, enhancing the albedo feedback. At the end of summer this feedback system resets as the air temperature decreases and surface melt reduces, and there is no more difference between the simulation scenarios. There is a lag in the time period needed for the cloud effect on the albedo to reset, which is presumably due to the fact that the lower latitudes still receive SW radiation in this time of year, maintaining the albedo feedback. For accumulation grid points, this feedback system is absent and the GrIS shows no long-term response to the cloud radiative forcing.

It appears that the LW radiation is not a significant factor for the long-term response of the GrIS to cloud forcing (supplementary figure S3). There is a small long-term warming of the GrIS of 0.9 $\pm$0.3°C for ablation grid points and practically none for accumulation grid points (0.03 $\pm$0.2°C). There is no certainty that this has significant effect on the surface melt (supplementary figure S4).

3.3 Impact on SMB

Eventually, the short-term and long-term effects of cloud radiation join forces. Table 1 shows that all-sky initialised simulations (AAI and CAI) have significantly more mass loss during the melt season than the clear-sky initialised scenarios (ACI and CCI), agreeing with the long-term cloud effect on the SWE in figure 2d. The increase in mass loss during the melt season from scenario ACI to AAI is 99.2 Gt/year, from scenario CCI to CAI this is 110.9 Gt/year (respectively 38.4% and 43.6%). Similar increases between the scenarios are found for the Melt-Area Index (MAI), which is the ratio between the area exposed to mass loss and the total area of the GrIS. This suggest that, during the melt season, the CRE influences mostly how much area is prone to mass loss. This can be traced back to the long-term response of the albedo to the cloud radiation, and the accompanying increase in net SW radiation (figure 2b and c). The MAI pleads that the

Table 1. Yearly averaged mass loss component of the SMB of the GrIS during the melt season and the corresponding Melt-Area Index, per simulation scenario in 2007-2010. All simulated days with a SMB < 0 are included when calculating mass loss, and account for meltwater runoff, sublimation and evaporation. SMB values are weighted for the respective areas of each gridpoint when calculating the representative value for the GrIS. The Melt-Area Index is the ratio between the area exposed to mass loss and the total area of the GrIS ($1.71 \cdot 10^6 km^2$) such that a high Melt-Area Index indicates a larger area exposed to mass loss.

scenario	#	SMB mass loss during melt season $[Gt/yr]$	Melt-Area Index $[-]$
AAI	1	357.2	139.7
CAI	2	365.3	149.2
ACI	3	258.0	102.6
CCI	4	254.4	105.3

CRE is more potent for priming areas to melt conditions than it is in amplifying the existing melt-rates, but note that this is not an explicit result.

Our results also show that clear-sky conditions on a single summer day produce more mass loss than a cloudy summer day: scenario CAI loses 8.1 Gt/year more during the melt season than scenario AAI, an increase of 2.3%. For scenario CCI with respect to ACI, it is an increase of 3.6 Gt/year (1.4%). This shows that relatively more incoming SW radiation (clear-sky) induces more melt, as Hofer et al. (2017) and Wang et al. (2018) have argued. But most prominently, these results demonstrate that such a clear-sky summer day yields the highest summer surface mass loss if it is initialised with all-sky conditions: scenario CAI yields much more mass loss than scenario CCI, agreeing with the findings of van Tricht et al. (2016).

Table 1, again, underlines the importance of on the long-term effect of cloud radiative forcing, on the one hand, and, on the other hand, the importance of the initial firn conditions when assessing cloud effects on glaciers and ice sheet.

4 Discussion

This study has succeeded in getting a step closer to understanding cloud radiative processes that are important for the GrIS SMB, bringing attention to the significance of the GrIS's long-term response. In particular, we show that the GrIS stores energy collected by a positive CRE, which decreases the albedo in the summer and enhances surface melt rates. The new firn's memory of the GrIS to cloud forcing implies that the conditions of the GrIS are essential for radiation studies on the SMB.

Moreover the positive long-term response of the GrIS to the CRE discloses the reason for the existing conflicting theories on the CRE. Wang et al. (2018) have studied the CRE using automatic weather stations and conclude that the CRE is negative at low albedo values and thus that clouds stabilise the albedo feedback and decelerate surface melt. Hofer et al. (2017) show that surface melt is governed by the decrease in albedo, but attribute this to decreasing cloud cover and thus indirectly to a negative CRE. Both these studies align with the short-term response of the GrIS to SW radiation. Complementary, this study now shows that the long-term GrIS response to SW radiation is positive and dominant in summer, not only agreeing with the findings of van Tricht et al. (2016) but indicating this as principal driver for surface melt and the cause for the dissimilarities between studies. Knowing this, we can conclude that radiation studies should not solely be based on observations but must be accompanied by a snow model.

Acknowledgments

The 2B-FLXHR-LIDAR data are available at http://www.cloudsat.cira.colostate.edu/. All codes that have contributed to the results of this study are available on request by the corresponding author.

References

Bintanja, R., & Van Den Broeke, M. (1996). The influence of clous on the radiation budget of ice and snow surfaces in antarctica and greenland summer. *International Journal of Climatology*, *16*(11), 1281-1296. doi: 10.1002/(SICI)1097-0088(199611)16:11⟨1281::AID-JOC83⟩3.0.CO;2-A

Box, J. E., Fettweis, X., Stroeve, J. C., Tedesco, M., Hall, D. K., & Steffen, K. (2012). Greenland ice sheet albedo feedback: thermodynamics and atmospheric drivers. *The Cryosphere*, *6*(4), 821–839. doi: 10.5194/tc-6-821-2012

Fettweis, X., Franco, B., Tedesco, M., van Angelen, J. H., Lenaerts, J. T. M., van den Broeke, M. R., & Galle, H. (2013). Estimating greenland ice sheet surface mass balance contribution to future sea level rise using the regional atmospheric climate model mar. *The Cryosphere*, *7*, 469489. doi: 10.5194/tc-7-469-2013

Fettweis, X., Hanna, E., Lang, C., Belleflamme, A., Erpicum, M., & Galle, H. (2013). Brief communication important role of the midtropospheric atmospheric circulation in the recent surface melt increase over the greenland ice sheet. *The Cryosphere*, *7*, 241-248. doi: 10.5194/tc-7-241-2013

Gardner, A. S., & Sharp, M. J. (2010). A review of snow and ice albedo and the development of a new physically based broadband albedo parameterization. *J. Geophys. Res.*, *115*, 1-15.

Hofer, S., Tedstone, A. J., Fettweis, X., & Bamber, J. (2017). Decreasing cloud cover drives the recent mass loss on the greenland ice sheet. *Sci. Adv.*, *3*(e1700584).

Lehning, M., Bartelt, P., Brown, B., Fierz, C., & Satyawali, P. (2002). A physical snowpack model for the swiss avalanche warning: part ii. snow microstructure. *Cold Regions Sci. Technol*, *35*, 147-167.

Noel, B. e. a. (2015). Evaluation of the updated regional climate model racmo2.3: summer snowfall impact on the greenland ice sheet. *The Cryosphere*, *9*, 1831-1844.

Shupe, M. D., & Intrieri, J. M. (2004). Cloud radiative forcing of the arctic surface: the influence of cloud properties, surface albedo, and solar zenith angle. *J. Clim.*, *17*, 616-628.

van Angelen, J. H. e. a. (2012). Sensitivity of greenland ice sheet surface mass balance to surface albedo parameterization: a study with a regional climate model. *The Cryosphere*, *6*, 1175-1186.

van den Broeke, M. R., Enderlin, E. M., Howat, I. M., Kuipers Munneke, P., Nol, B. P., Jan Van De Berg, W., ... Wouters, B. (2016). On the recent contribution of the greenland ice sheet to sea level change. *The Cryosphere*, *10*, 19331946. doi: 10.5194/tc10-1933-2016

van Tricht, K., Lhermitte, S., Lenaerts, J., Gorodetskaya, I., L'Ecuyer, T., Noel, B., ... van Lipzig, N. (2016). Clouds enhance greenland ice sheet meltwater runoff. *Nat. Commun*, *7:10266*. doi: 10.1038/ncomms10266

Wang, W., Zender, C., & As, D. (2018). Temporal characteristics of cloud radiative effects on the greenland ice sheet: Discoveries from multiyear automatic weather station measurements. *Journal of Geophysical Research: Atmospheres*, *0*(0). doi: 10.1029/2018JD028540

Supporting Information for "Greenland Ice Sheet Memory for Cloud Radiation determines its impact on the Surface Mass Balance"

M. Izeboud[1], S. Lhermitte[1], K. Van Tricht[2], J.T.M. Lenaerts[3], N. Van Lipzig[4], N. Wever[3]

[1]Delft University of Technology, Department of Geoscience and Remote Sensing

[2]VITO Remote Sensing, Mol, Belgium

[3]Department of Atmospheric and Oceanic Sciences, University of Colorado Boulder, Boulder CO, USA

[4]KU Leuven

[1]Stevinweg 1, 2628CN Delft, The Netherlands

[2]Boeretang 200, 2400 Mol, Belgium

[3]311 UCB, Boulder, Colorado, 80309-0311, United States of America

[4]Oude Markt 13, 3000 Leuven, Belgium

Contents of this file

Corresponding author: M.Izeboud, Department of Geoscience Remote Sensing, Delft University of Technology, Stevinweg 1, Delft, 2628 CN, The Netherlands. (maaike.izeboud@live.nl)

Introduction

This document includes additional figures, to add to the argumentation in the main article.

Figures S1. See figures below. Captions contain all the necessary explanation per figure, for thorough understanding refer to the main article. For clarity, the overview of abbreviations used to name different scenarios is included here as well as in the main article:

1. AAI: one all-sky day simulated, initialised with preceding all-sky conditions.
2. CAI: one clear-sky day simulated, initialised with preceding all-sky conditions.
3. ACI: one all-sky day simulated, initialised with preceding clear-sky conditions.
4. CCI: one clear-sky day simulated, initialised with preceding clear-sky conditions.

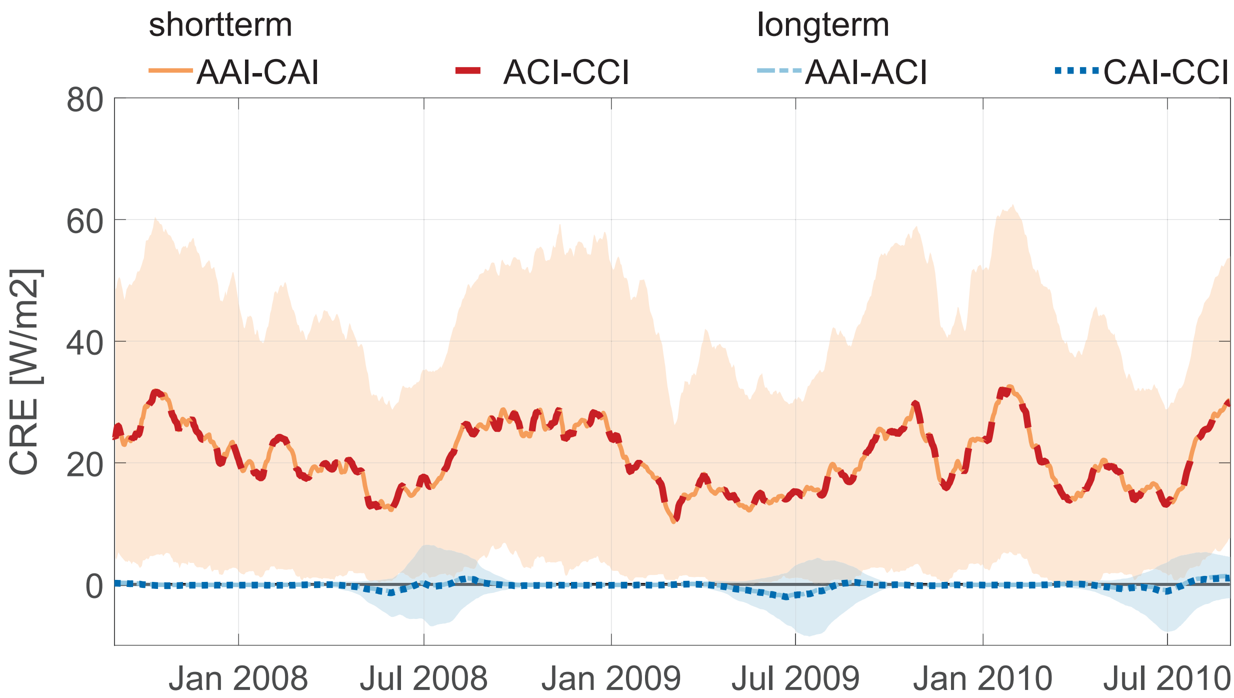

Figure S1. Cloud radiative effect (CRE) on the GrIS for only accumulation gridpoints. Time-series of both short term (red lines, scenario AAI-CAI and ACI-CCI) and long term (blue lines, scenario AAI-ACI and CAI-CCI) CRE. Plotted with a 30-day moving average. The shaded areas represent the 10 to 90 percentile of the accumulation gridpoint data.

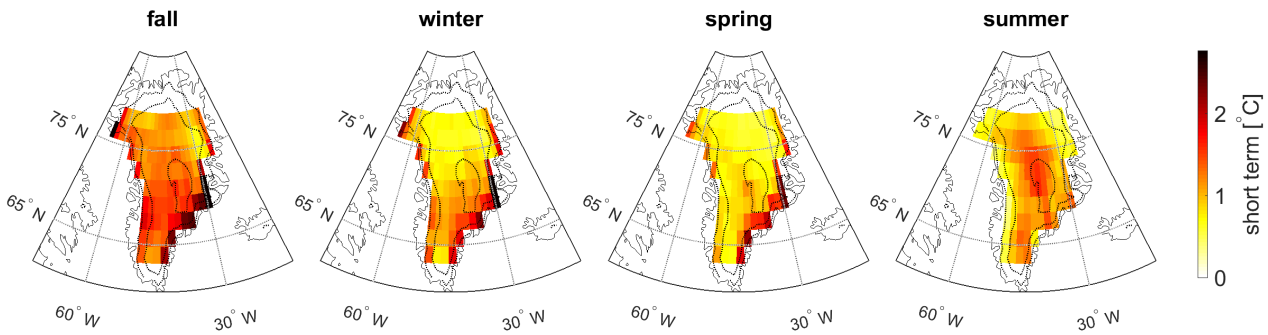

Figure S2. Short term cloud radiative effect on the GrIS surface temperature. Averaged difference between scenario AAI-CAI and ACI-CCI over 2007-2010. Values per grid point are seasonal averages.

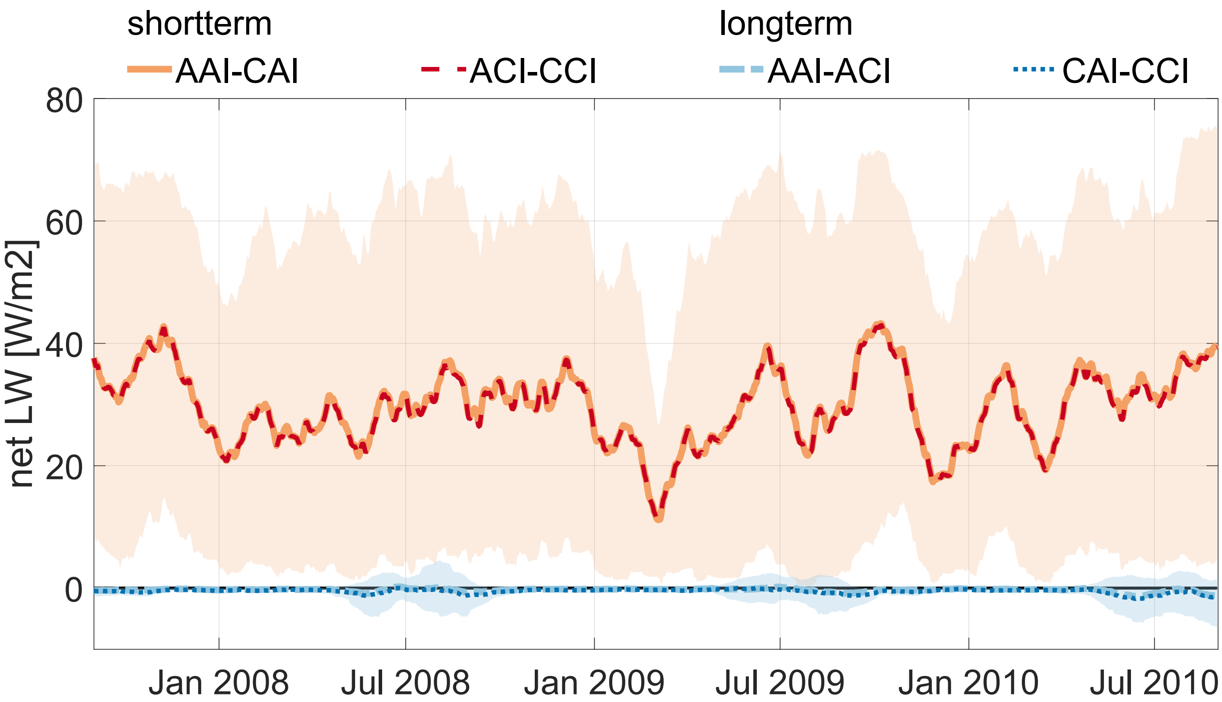

Figure S3. Cloud radiative effect (CRE) on the GrIS net longwave radiation budget. Time-series of both short term (red lines, scenario AAI-CAI and ACI-CCI) and long term (blue lines, scenario AAI-ACI and CAI-CCI) CRE, for only ablation grid points. Plotted with a 30-day moving average. The shaded areas represent the 10 to 90 percentile of the ablation gridpoint data.

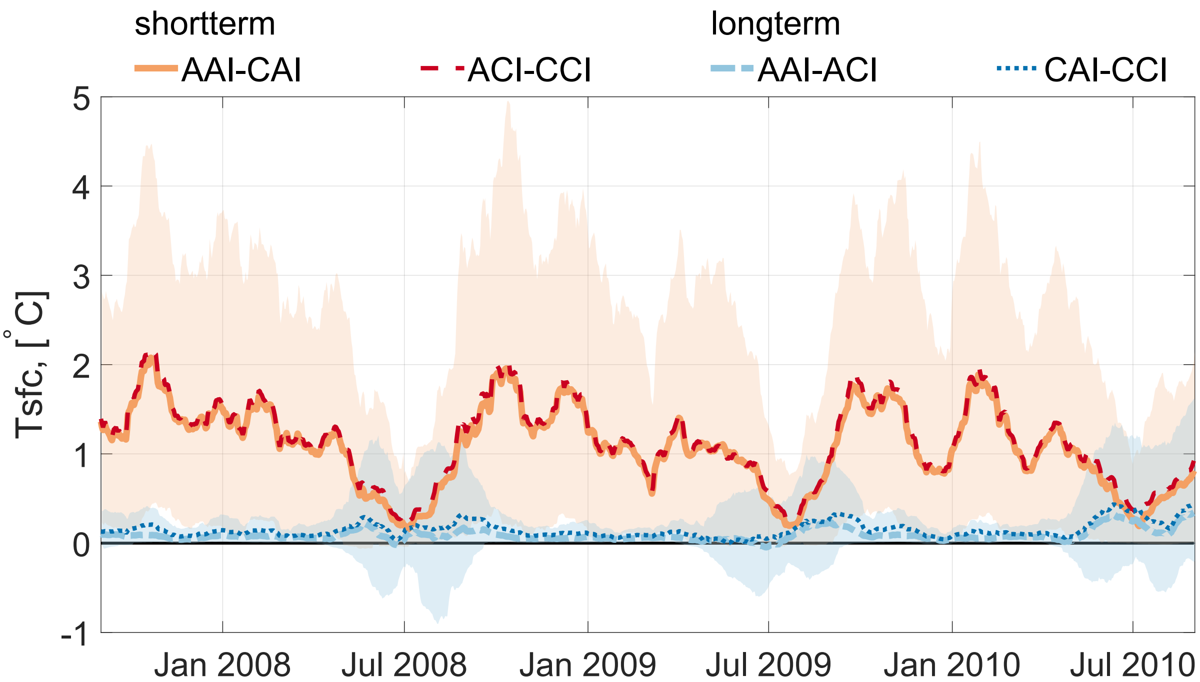

Figure S4. Cloud radiative effect (CRE) on the GrIS surface temperature. Time-series of both short term (red lines, scenario AAI-CAI and ACI-CCI) and long term (blue lines, scenario AAI-ACI and CAI-CCI) CRE, for only ablation grid points. Plotted with a 30-day moving average. The shaded areas represent the 10 to 90 percentile of the ablation gridpoint data.